nature climate change

LETTERS

PUBLISHED ONLINE: 4 MAY 2014 | DOI: 10.1038/NCLIMATE2226

Ice plug prevents irreversible discharge from East Antarctica

M. Mengel[1,2] and A. Levermann[1,2]*

Changes in ice discharge from Antarctica constitute the largest uncertainty in future sea-level projections, mainly because of the unknown response of its marine basins[1]. Most of West Antarctica's marine ice sheet lies on an inland-sloping bed[2] and is thereby prone to a marine ice sheet instability[3–5]. A similar topographic configuration is found in large parts of East Antarctica, which holds marine ice equivalent to 19 m of global sea-level rise[6], that is, more than five times that of West Antarctica. Within East Antarctica, the Wilkes Basin holds the largest volume of marine ice that is fully connected by subglacial troughs. This ice body was significantly reduced during the Pliocene epoch[7]. Strong melting underneath adjacent ice shelves with similar bathymetry[8] indicates the ice sheet's sensitivity to climatic perturbations. The stability of the Wilkes marine ice sheet has not been the subject of any comprehensive assessment of future sea level. Using recently improved topographic data[6] in combination with ice-dynamic simulations, we show here that the removal of a specific coastal ice volume equivalent to less than 80 mm of global sea-level rise at the margin of the Wilkes Basin destabilizes the regional ice flow and leads to a self-sustained discharge of the entire basin and a global sea-level rise of 3–4 m. Our results are robust with respect to variation in ice parameters, forcing details and model resolution as well as increased surface mass balance, indicating that East Antarctica may become a large contributor to future sea-level rise on timescales beyond a century.

Sea-level rise is a major consequence of climatic warming and impacts coastal areas through increased risk of flooding worldwide[9]. Improved sea-level projections are required for global and regional adaptation strategies[10].

Most recent work on Antarctica's sea-level contribution concentrated on West Antarctica's Amundsen sector where the grounding line is retreating[11,12] and large regions of ice are grounded below sea level on an inland-sloping bed. This topographic situation was shown to be potentially unstable[4], even when stabilizing effects of marginal stresses and bottom topography are accounted for[13,14]. As the East Antarctic ice sheet holds a multiple volume of marine-based ice as compared with West Antarctica[6], the understanding of East Antarctica's marine ice sheet dynamics is key to better determine Antarctica's future contribution to sea-level changes.

The vast Wilkes subglacial basin is located west of the Transantarctic Mountains and is drained through the Ninnis and Cook ice streams[15] at George V Coast (Fig. 1). As revealed by recently improved bed topography data[6], the Wilkes ice sheet rests on two deep troughs that are the remnants of larger palaeo-streams. The troughs' shape (Fig. 2b) implies a deeper-lying grounding line if the ice recedes from its present position, with the potential of an instability with increased ice flux[4].

Further west at the neighbouring Wilkes coast strong thermal forcing is observed under the Totten and Moscow University ice shelves and has been suggested to cause the imbalance of Totten Glacier with thinning rates up to 1.9 m yr^{-1} observed at present[16]. Although there is no evidence for a present large-scale imbalance of the Cook and Ninnis glaciers—reported thinning rates range from $\sim$0.025 m yr^{-1} (ref. 17) to $\sim$0.15 m yr^{-1} (ref. 18)—the similar regional bathymetry in principle allows for warm modified Circumpolar Deep Water to access the Ninnis and Cook grounding lines. The observed low melting rate and low melting-to-calving ratio[8] indicates that heat transport to the grounding line is not excessive although a downstream freshening off the Adélie coast may be attributed to Cook shelf melting[19].

During the mid- to late Pliocene (4.8–3.5 million years ago) massive ice discharge occurred from the unstable margins of Adélie and Wilkes Land due to ice-stream surges that were linked to rapid grounding-line retreat during a warming climate[20]. Marine sediment cores from offshore Adélie land include continental bedrock from the interior of the Wilkes subglacial basin[7]. As active erosion zones lie close to the margin of the ice sheet, the Pliocene, featuring temperature and CO_2 levels similar to end-of-this-century projections, may have had a significantly smaller ice sheet in East Antarctica's Wilkes Basin, posing the question of the stability of its present marine-based ice.

Here we explore this stability using regional simulations with the Parallel Ice Sheet Model (PISM; Methods) and appropriate boundary conditions. PISM applies the superposition of two shallow approximations to consistently simulate slowly moving grounded ice and the fast-flowing ice of outlet glaciers, ice streams and ice shelves[21]. The transition zone between sheet and shelf is not parametrized and can fully adapt to changes in ice flow and geometry. The local interpolation of grounding-line position and basal friction and a specific driving stress scheme at the grounding line make PISM capable of modelling reversible grounding-line motion in the Mismip3d experiments[22] comparable to the results obtained from full-Stokes flow[23].

We start from an ensemble of stable equilibrium states, created through the perturbation of ice-flow and basal-friction parameters under time-constant present-day atmosphere and ocean boundary conditions[24,25] (Supplementary Table 1). Model domain boundaries lie at present ice divides surrounding the drainage basin[15] and are far from the main ice-dynamical changes induced by the forcing (Fig. 1). The coastal ice margin at George V Coast is free to evolve in the Pacific sector of the Southern Ocean. We force the ice sheet's equilibrium states with warm water pulses by raising the ocean temperature beneath the ice shelves to 1°–2.5 °C above the values applied during equilibrium (Supplementary Table 2). The pulses have a length between 200

[1]Potsdam Institute for Climate Impact Research, 14412 Potsdam, Germany, [2]Institute of Physics, Potsdam University, 14476 Potsdam, Germany.
*e-mail: anders.levermann@pik-potsdam.de

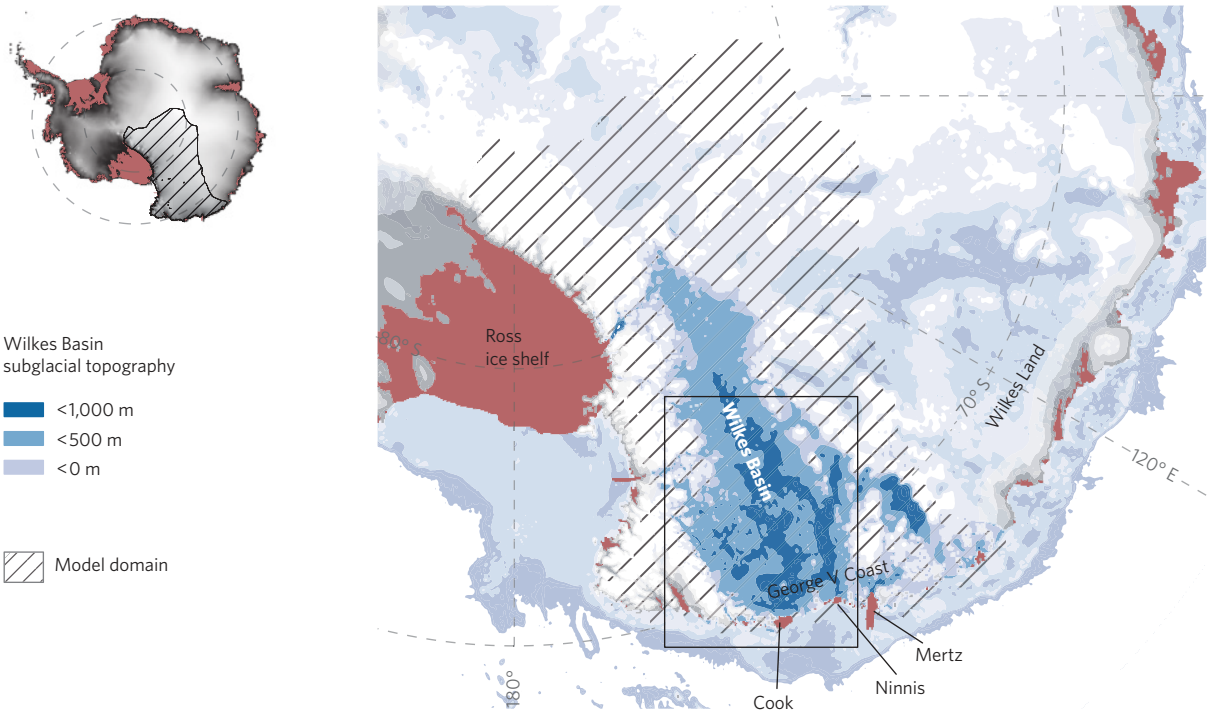

Figure 1 | The Wilkes Basin; subglacial area and model domain. The Wilkes Basin (labelled blue shadings) is the largest region with topography below sea level in East Antarctica. At George V Coast, the Cook and Ninnis ice streams drain into the Southern Pacific Ocean and rest on deep palaeo-troughs[6]. Our model domain (hatches) extends to the present ice divides[15]. The rectangle refers to the region shown in Fig. 2.

and 800 years. Owing to the cold equilibrium conditions in the vicinity of the ice shelves, water temperatures never exceed 0.3 °C in any of the forcing experiments (Methods). We explore the ice sheet's evolution under the subsequently unperturbed equilibrium boundary conditions.

A small volume of ice (to be referred to as the 'ice plug') is the deciding factor for the stability of the marine-based ice in our simulations. Self-sustaining retreat occurs in model simulations that eliminate this plug (Fig. 2a,b, total red area), whereas the system is stable if the plug is sustained after the forcing has ended. We characterize the ice-plug volume by the sea-level-relevant ice that is lost from the state observed at present[6] in the region (Fig. 3, x axis). Stabilization is certain for ice loss below 60 mm in sea-level equivalent (sleq). Stable and unstable states coexist for ice loss between 60 mm sleq (22,200 Gt) and 80 mm sleq (29,600 Gt). Beyond the threshold of 80 mm, only unstable states exist and the ice sheet enters a phase of self-sustained retreat in all of our simulations. The two regimes of a stable (blue points in Fig. 3) and an unstable ice sheet (red points) exist for all parameter combinations that we explored with 7 km (Fig. 3, coloured points) and 10 km (grey points) horizontal resolution, leading to a threshold dependence on the initial ice loss.

The unstable ice sheet retreats under unperturbed boundary conditions towards a new equilibrium that lies in a region that is covered by up to 2.5-km-thick ice at present (Fig. 2a,b, thick grey contours). This causes sea-level rise between 3 and 4 m (Figs 3 and 4a y axis). The main retreat occurs on a timescale of 10 kyr and the grounding line stabilizes after 25 kyr in all experiments (Fig. 4). The expected rate of sea-level rise from the Wilkes Basin has an upper bound of 0.5 mm yr^{-1} (Supplementary Fig. 1). This is twice the rate of Antarctica's present total contribution to sea-level rise[1]. Considering the necessary forcing time of 200 years and longer (Supplementary Table 2), the Wilkes marine-based ice may therefore significantly modulate the sea-level signal on timescales longer than a century whereas our results suggest that the implications of the instability for short-term sea-level rise are limited.

In agreement with one-dimensional theoretical results[4], the instability is induced only if the grounding line reaches the deep troughs behind the ice plug (Fig. 2b, red contour) during the forcing, leading to a strong increase in ice flow across the grounding line. In our experiments the retreat occurs fastest in the deepest regions of the basin and decelerates on subglacial ridges (Fig. 2a,b, thin grey contours). The ice sheet does not stabilize at the position of deepest topography, but further inland. This is consistent with the grounding-line motion being dominated by the flux imbalance between grounding-line flow and hinterland, but also with the one-dimensional theoretical results. Within this theory the region upstream of the ice plug with a deeper, yet flat bed can be considered as metastable.

The complete discharge of the Wilkes Basin occurs only when the grounding-line flux is complemented by sufficient volume loss of the ice shelf. This relates the response timescale of the upstream ice flux to the timescale of the applied forcing as demonstrated by the resilience to weaker and longer forcing (1.2 °C, 800 yr, Supplementary Table 2 experiment 1) in contrast to the instability under the stronger but shorter forcing (1.8 °C, 400 yr, experiment 4). Although the total ice loss through melting exceeds that of the unstable 400-year experiments by a factor of 1.13, the ice sheet stabilizes in the 800-year experiment. That is because the ice flow from the hinterland has time to adapt and balance the melting-induced loss. The Wilkes marine-based ice may therefore be more vulnerable to fast changes in ocean heat supply than to more gradual ones.

The total subshelf melting during the forcing period varies between 120 Gt yr^{-1} and 250 Gt yr^{-1}. The corresponding heat flux of 1.3 TW–2.6 TW is comparable to estimates for the present heat flux into the Amundsen embayment[26] and towards the Dotson and Getz ice shelves[27]. The applied forcing is therefore consistent with a significant but not unrealistic change in the ocean circulation that

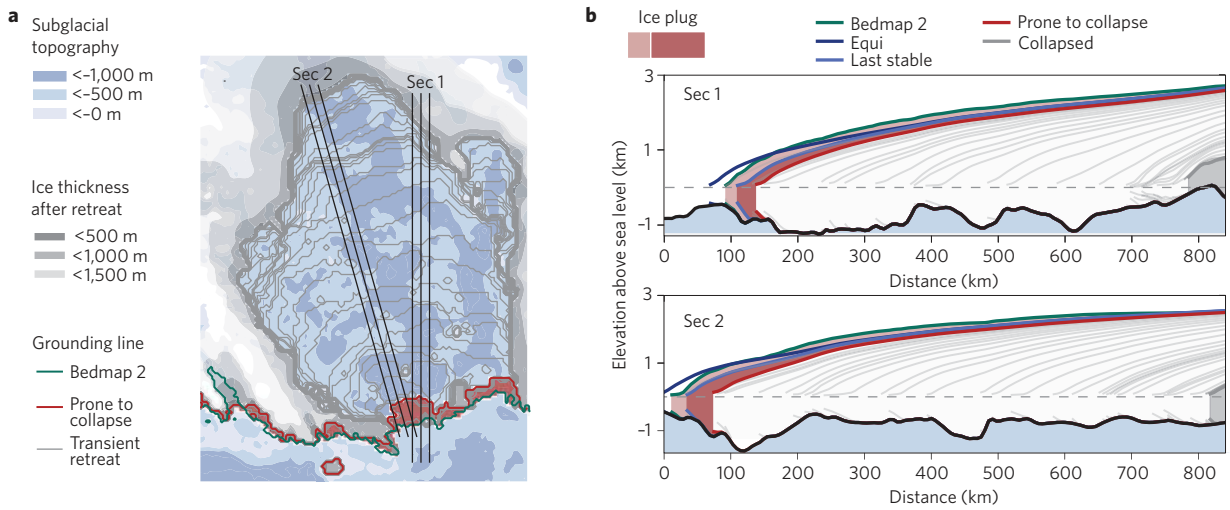

Figure 2 | The ice plug. Difference between stable and unstable states, defining the ice plug. **a**, Area of ungrounded ice compared to observed data[6] as red shading (ice-plug area), grounding line of the observed[6] (green contour) and the unstable state (red contour). **b**, Cross-section through the two main troughs. Observed ice topography[6] (green), modelled equilibrium (dark blue), last stable (blue) and unstable (red) state and the difference between observed and last stable (light red shading) and last stable and unstable simulation (dark red shading). Light grey contours indicate the transient grounding line (left) and ice topography (right) in intervals of 800 yr starting after the plug removal. Based on the 7 km resolution (see Supplementary Table 2 for details).

continuously supplies heat to the grounding line in a similar amount as observed at present in West Antarctica.

How robust is the instability to uncertainties in the boundary conditions? The ice shelves have to compensate the mass they absorb from grounding-line flux by calving and subshelf melting. As the melting is pressure-dependent, it dominates the ice loss during the fast retreat in the deep troughs, necessitating heat fluxes of the order of 0.5 TW in total. The ice shelf melting during the retreat into the basin depends on unknown ocean conditions that we needed to estimate (Methods). We verified the self-sustaining retreat to be still present, albeit slower, under colder ocean conditions similar to today's large shelves.

Future atmospheric warming is projected to increase moisture transport to the Antarctic ice sheet roughly following the Clausius–Clapeyron law[28]. To test the robustness of our results to varying surface mass balance, we apply a 30%-snowfall increase during the ocean forcing and the subsequent response phase. Such an increase has been projected for the end of the twenty-second century under the A1B scenario[28]. Applying it for the full period serves as an upper bound of the snowfall effect. The threshold as shown in Fig. 3 is reproduced under increased snowfall (Supplementary Fig. 2). The ice-plug volume (Supplementary Fig. 2, x axis) integrates both changes in surface mass balance and dynamic ice loss through melting. Ice loss is around one order of magnitude larger than the $\sim 10\,\mathrm{Gt\,yr^{-1}}$ ice gain by additional accumulation in the plug region. Therefore, only the experiments closest to the threshold stabilize through increased surface accumulation and move to the lower left (Supplementary Fig. 2, blue rectangles), which does not alter the threshold itself. Even over a period of 20 kyr and longer, the ice loss from self-sustained retreat strictly dominates over the mass gain from increased snowfall in the region, leading to sea-level rise of around 3 m (Supplementary Fig. 2, y axis). Owing to the lack of an interactive surface-mass-balance model our results, however, neglect any feedback through changes in ice geometry.

The specific topographic configuration with a small ice plug on a ridge and a large subglacial basin that expands inland makes the Wilkes ice sheet susceptible to a self-sustained ice-sheet retreat. A similar mechanism has initiated the ongoing retreat of Pine Island Glacier, which detached from a subglacial ridge in the 1970s (ref. 12). The unstable ice covering the Wilkes Basin in East Antarctica may play a significant role in future long-term sea-level rise and may help to explain the gap between palaeo-shoreline data and the sea-level contribution that can be expected from a significant ice loss of West Antarctica and Greenland.

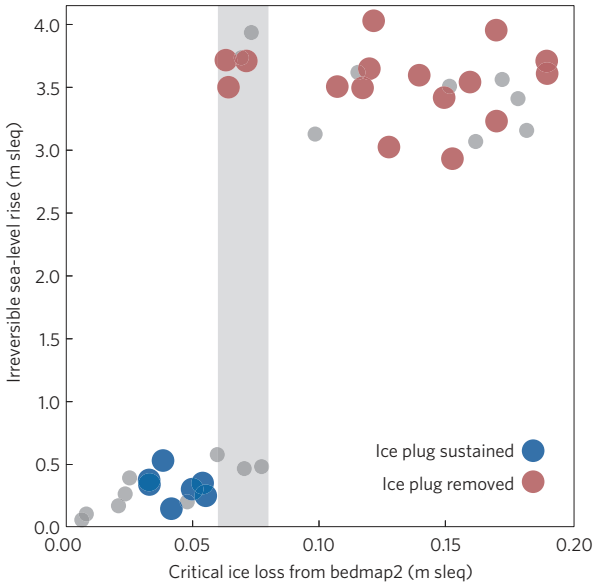

Figure 3 | Collapse condition. Long-term sea-level rise as a function of the ice volume removed from the state observed at present in the plug region. Stable states (blue) exist only below the threshold that corresponds to approximately 60 mm sea-level-relevant ice loss from the ice-plug region. The unstable states (red) feature self-sustained long-term sea-level rise of 3–4 m, defined as the sea-level-relevant ice loss 25 kyr after the forcing ended. All coloured dots are based on 7 km resolution, grey dots are based on 10 km resolution.

Methods

We use PISM (refs 21,29) to carry out regional simulations on 7 km and 10 km resolution. Our hybrid shallow approximation ensures stress transmission across the grounding line and a smooth transition between regimes of fast-flowing,

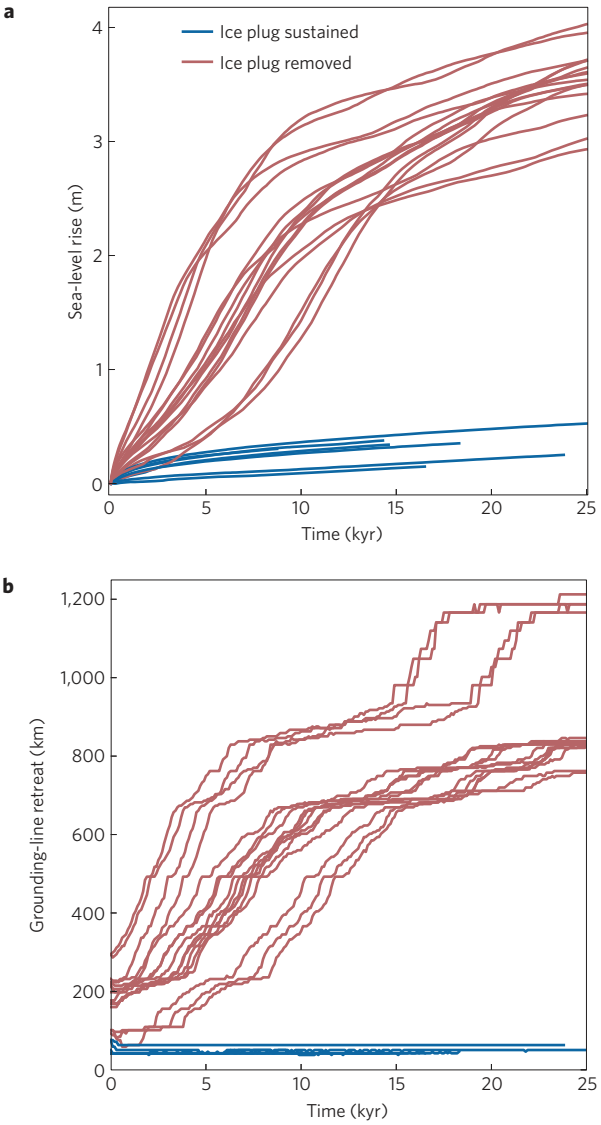

Figure 4 | Transient sea-level contribution and grounding-line retreat after the end of the forcing. a,**b**, Sea-level contribution (**a**) and grounding-line retreat (**b**) of stable (blue) and unstable (red) states after the end of the forcing. Sea-level change as anomaly to the end-of-forcing value. Grounding-line retreat along section 2 as depicted in Fig. 2. Stable (blue) and unstable (red) states were determined before the evolution shown here by use of the ice-plug condition (Fig. 3 *x* axis, colours related). All simulations were run on 7 km resolution.

sliding and slowly deforming, bedrock-frozen ice. The grounding line can freely evolve also under lower resolution owing to a local interpolation of the grounding-line position that affects the basal friction and a new driving stress scheme at the grounding line. The interpolation leads to reversible grounding-line dynamics that is consistent with full-Stokes simulations in high resolution[23]. The response time to external perturbations on decadal timescales deviates from the full-Stokes simulations by a factor of around two[23]. Compared with these decadal-scale perturbations, the relevant dynamics in this study occur on timescales that are one order of magnitude slower, that is, on centennial timescales and below. We therefore expect only minor influence on our results.

Model boundaries lie on present drainage divides[15] and are far from the region of self-sustained retreat. Boundary velocities are zero for the drainage divides and taken from observations[15] for the glaciers draining through the Transantarctic Mountains. The fixed boundaries may lead to a slight underestimation of the equilibrated ice loss from the unstable simulations because no ice can be drained from neighbouring basins.

We ran the model under constant ocean and atmosphere boundary conditions for at least 40 kyr to generate the equilibrium states that serve as starting points for our forcing experiments (Supplementary Table 1). We sampled a three-dimensional parameter space to capture the core uncertainty in ice flow and basal sliding by variation of the two enhancement factors for the shallow-ice approximation and the shallow-shelf approximation as well as the basal till pore-water pressure. The maximum deviation of ice volume from observations is less than 8% for the total domain and less than 20% for the plug region. The ice plug (Fig. 3, *x* axis) is defined as the difference from the observed volume and therefore the equilibrium deviation does not directly affect the determined threshold.

Subshelf melting is calculated from ocean-model temperature and salinity data solving a three-equation system[30] for the boundary layer beneath the ice shelf as also applied in at least two dynamic Southern Ocean models. The parametrization is detailed in the Supplementary Information.

The equilibrium simulations are forced with time-constant ocean data from the BRIOS (ref. 25) model, leading to typical temperatures of −1.8 °C at the ice–ocean interface (Supplementary Fig. 3). We enforce the ice-mass loss from the George V coast by warm water anomalies from 1.0 to 2.5 °C and periods of 200–800 years. The resulting subshelf melting, boundary-layer temperature and boundary-layer salinity are illustrated in Supplementary Fig. 4. The forcing time and strength that is sufficient to remove the ice plug depends on the ice-model parameters. Details are given in Supplementary Table 2. We integrated all forcing experiments for at least 25 kyr after the forcing ended so that a stable grounding line was reached.

As oceanic conditions in regions covered at present by land ice are unknown, we filled missing ocean data by simple diffusion along regions below sea level, leading to water properties in the Wilkes subglacial basin similar to today's George V coast. Salinity may deviate from observations in the model data we use. However, the sensitivity of subshelf melting to salinity is relatively weak (Supplementary Fig. 5).

Atmospheric boundary conditions are taken from observations[24]. We test the sensitivity to the potential future increase of surface accumulation by scaling the pattern observed at present with a factor of 1.3.

Received 21 November 2013; accepted 1 April 2014; published online 4 May 2014

References

1. Church, J. A. *et al.* in *Climate Change 2013: The Physical Science Basis* (eds Stocker, T. *et al.*) (Cambridge Univ. Press, 2013).
2. Bamber, J. L., Riva, R. E. M., Vermeersen, B. L. A. & LeBrocq, A. M. Reassessment of the potential sea-level rise from a collapse of the West Antarctic ice sheet. *Science* **324,** 901–903 (2009).
3. Mercer, J. H. West Antarctic ice sheet and CO_2 greenhouse effect: A threat of disaster. *Nature* **271,** 321–325 (1978).
4. Schoof, C. Ice sheet grounding line dynamics: Steady states, stability, and hysteresis. *J. Geophys. Res.* **112,** F03S28 (2007).
5. Pollard, D. & DeConto, R. M. Modelling West Antarctic ice sheet growth and collapse through the past five million years. *Nature* **458,** 329–332 (2009).
6. Fretwell, P. *et al.* Bedmap2: Improved ice bed, surface and thickness datasets for Antarctica. *Cryosphere* **7,** 375–393 (2013).
7. Cook, C. P. *et al.* Dynamic behaviour of the East Antarctic ice sheet during Pliocene warmth. *Nature Geosci.* **6,** 765–769 (2013).
8. Rignot, E., Jacobs, S., Mouginot, J. & Scheuchl, B. Ice-shelf melting around Antarctica. *Science* **341,** 266–270 (2013).
9. Hirabayashi, Y. *et al.* Global flood risk under climate change. *Nature Clim. Change* **3,** 816–821 (2013).
10. Nicholls, R. J. & Cazenave, A. Sea-level rise and its impact on coastal zones. *Science* **328,** 1517–1521 (2010).
11. Payne, A. J., Vieli, A., Shepherd, A. P., Wingham, D. J. & Rignot, E. Recent dramatic thinning of larges West Antarctic ice stream triggered by oceans. *Geophys. Res. Lett.* **31,** http://dx.doi.org/10.1029/2004GL021284 (2004).
12. Jenkins, A. *et al.* Observations beneath Pine Island Glacier in West Antarctica and implications for its retreat. *Nature Geosci.* **3,** 468–472 (2010).
13. Hindmarsh, R. C. A. The role of membrane-like stresses in determining the stability and sensitivity of the Antarctic ice sheets: Back pressure and grounding line motion. *Phil. Trans. R. Soc.* **364,** 1733–1767 (2006).
14. Favier, L. *et al.* Retreat of Pine Island Glacier controlled by marine ice-sheet instability. *Nature Clim. Change* **4,** 117–121 (2014).
15. Rignot, E., Mouginot, J. & Scheuchl, B. Ice flow of the Antarctic ice sheet. *Science* **333,** 1427–1430 (2011).
16. Pritchard, H. D., Arthern, R. J., Vaughan, D. G. & Edwards, L. A. Extensive dynamic thinning on the margins of the Greenland and Antarctic ice sheets. *Nature* **461,** 971–975 (2009).
17. Velicogna, I. & Wahr, J. Time-variable gravity observations of ice sheet mass balance: Precision and limitations of the GRACE satellite data. *Geophys. Res. Lett.* **40,** 3055–3063 (2013).

18. Flament, T. & Rémy, F. Dynamic thinning of Antarctic glaciers from along-track repeat radar altimetry. *J. Glaciol.* **58,** 830–840 (2012).
19. Aoki, S. *et al.* Widespread freshening in the seasonal ice zone near 140° E off the Adélie Land Coast, Antarctica, from 1994 to 2012. *J. Geophys. Res. Ocean.* **118,** 6046–6063 (2013).
20. Williams, T. *et al.* Evidence for iceberg armadas from East Antarctica in the Southern Ocean during the late Miocene and early Pliocene. *Earth Planet. Sci. Lett.* **290,** 351–361 (2010).
21. Bueler, E. & Brown, J. The shallow shelf approximation as a sliding law in a thermomechanically coupled ice sheet model. *J. Geophys. Res.* **114,** F03008 (2009).
22. Pattyn, F. *et al.* Grounding-line migration in plan-view marine ice-sheet models: Results of the ice2sea MISMIP3d intercomparison. **59,** 410–422 (2013).
23. Feldmann, J., Albrecht, T., Khroulev, C., Pattyn, F. & Levermann, A. Resolution-dependent performance of grounding line motion in a shallow model compared to a full-Stokes model according to the MISMIP3d intercomparison. *J. Glaciol.* **60,** 353–360 (2014).
24. Comiso, J. C. Variability and trends in antarctic surface temperatures from *in situ* and satellite infrared measurements. *J. Clim.* **13,** 1674–1696 (2000).
25. Timmermann, R., Beckmann, A. & Hellmer, H. H. Simulations of ice-ocean dynamics in the Weddell Sea 1 Model configuration and validation. *J. Geophys. Res.* **107,** 10-1–10-11 (2002).
26. Walker, D. P. *et al.* Oceanic heat transport onto the Amundsen Sea shelf through a submarine glacial trough. *Geophys. Res. Lett.* **34,** L02602 (2007).
27. Ha, H. K. *et al.* Circulation and modification of warm deep water on the central Amundsen Shelf. *J. Phys. Oceanogr.* http://dx.doi.org/10.1175/JPO-D-13-0240.1 (2014).
28. Ligtenberg, S. R. M., Berg, W. J., Broeke, M. R., Rae, J. G. L. & Meijgaard, E. Future surface mass balance of the Antarctic ice sheet and its influence on sea level change, simulated by a regional atmospheric climate model. *Clim. Dynam.* **41,** 867–884 (2013).
29. Winkelmann, R. *et al.* The Potsdam Parallel Ice Sheet Model (PISM–PIK)–Part 1: Model description. *Cryosphere* **5,** 727–740 (2011).
30. Hellmer, H. H., Jacobs, S. S. & Jenkins, A. in *Ocean, Ice, and Atmosphere: Interactions at the Antarctic Continental Margin* (eds Jacobs, S. & Weiss, R.) 319–339 (Antarctic Research Series, Vol. 75, American Geophysical Union, 1998).

Acknowledgements

The study was partially financially supported by the German Federal Ministry of Education and Research (BMBF) and the German Environmental Foundation (DBU). We thank R. Timmermann and H. Hellmer for providing ocean model data for temperature and salinity. Model development for PISM at the University of Alaska, Fairbanks, USA was supported by the NASA grants NNX09AJ38C, NNX13AM16G and NNX13AK27G.

Author contributions

M.M. and A.L. designed the study and wrote the text. M.M. conducted the model simulations and prepared the figures.

Additional information

Supplementary information is available in the online version of the paper. Reprints and permissions information is available online at www.nature.com/reprints. Correspondence and requests for materials should be addressed to A.L.

Competing financial interests

The authors declare no competing financial interests.